

## Studies in Epilepsy Patients using Simultaneous PET/MR: Preliminary Results

Yu-Shin Ding<sup>1,2</sup>, Bangbin Chen<sup>3</sup>, Christopher Glielmi<sup>4</sup>, Timothy Shepherd<sup>1</sup>, Thomas Koesters<sup>1</sup>, Anne-Kristin Vahle<sup>1</sup>, Kent Friedman<sup>1</sup>, Fernando Boada<sup>1</sup>, and Orrin Devinsky<sup>5</sup>

<sup>1</sup>Radiology, New York University School of Medicine, New York, NY, United States, <sup>2</sup>Psychiatry, New York University School of Medicine, New York, NY, United States,

<sup>3</sup>Medical Imaging, National Taiwan University Hospital, Taiwan, <sup>4</sup>Siemens Healthcare, NY, United States, <sup>5</sup>Neurology, New York University School of Medicine, NY, United States

**Background:** Functional neuroimaging techniques, including positron emission tomography (PET), single-photon emission computerized tomography (SPECT), magnetic resonance spectroscopy (MRS), and functional magnetic resonance imaging (fMRI), can be very useful in the localization of the epileptogenic zone and for mapping functional areas of the brain. A combined PET/MR scanner with simultaneous acquisition permits simultaneous imaging of physiologic & pathophysiological processes and provides both anatomical & functional information on the same subject at the same time. It allows direct correlations of PET data with MR-detected patterns of neural synchrony in both grey and white matters; e.g. resting-state fMRI, diffusional kurtosis imaging, and MRS. This multi-modal analysis will facilitate the identification of an optimal biomarker. To demonstrate feasibility of this, we initiated a comparative study in neurotypical controls (NC) and epilepsy patients (Epi) using F-18-fluorodeoxyglucose (FDG). In this report, quantitative data analysis on glucose metabolism in over 120 brain regions is compared between two groups. Correlations of FDG uptake to MR findings for specific regional abnormality in patients are also explored.

**Methods:** Six NC and 11 Epi patients (avg. age 26 and 36, respectively) were imaged on a whole-body simultaneous PET/MR scanner (Biograph mMR, Siemens). After injection of approx. 370 MBq FDG, dynamic brain PET scans were acquired for ~90 minutes. Simultaneously, MR imaging, including T1, T2, resting state, DKI, MRS, field map and other sequences, were performed. Dixon sequence was acquired to obtain a  $\mu$ -map for attenuation correction (AC) of PET data. Standard uptake values (SUV) were mapped via MATLAB on a summed PET image (127 slices) of each subject. A total of 117 masks (regions of interest, ROIs), including left and right, for cortical (96) and subcortical regions (21) based on Harvard-Oxford Atlas were generated. Image preprocessing was carried out using Mango and FSL. The SUV maps were registered to the subject's T1 images that, in turn, are registered to the MNI152 2mm template. After applying the masks, averaged SUV values for all masks were derived for all subjects. Statistical analyses on SUV values derived from two normalization methods, by individual subject's mean cortical SUV ( $SUV_{COR\_norm}$ ) or by white matter ( $SUV_{WM\_norm}$ ), were compared.

**Results:** Based on Mann-Whitney U test (SPSS) and pair-t-tests, ROIs (masks) that showed significant difference between two groups are tabulated in **Table 1**.  $SUV_{COR\_norm}$  values showed more hypometabolic regions and more asymmetry regions in Epi patients than NC, compared to  $SUV_{WM\_norm}$  values. The same ROIs showing the significant difference that rendered by both methods are (1) hypermetabolism (Epi > NC): Middle Frontal gyrus\_R, Precentral Gyrus\_R, Postcentral Gyrus\_L&R, Superior Parietal Lobule\_L (i.e., masks 8, 14, 33&34, 35); (2) hypometabolism (Epi < NC): Temporal Pole\_R (mask16) and Planum Polare (mask 87, anterior portion of the superior surface of the temporal lobe); (3) more ROIs for Epi than NC with SUV difference between right and left. Locations of selected masks that showed group significance are shown in **Fig. 1**. **Fig. 2** shows FDG overlaid (bottom row) on coronal T2 FLAIR (top row) for an epilepsy patient with left hippocampal sclerosis, showing good correlation of hypometabolism in the lesion area, which was further confirmed by time-activity curves of this patient vs. a matched control (Fig. 3).

**Table 1.** Compare SUV value between healthy control and epilepsy patients (6 NC, 11 Epi Pt)

Metabolism	$SUV_{WM\_norm}$	P value	$SUV_{COR\_norm}$	P value
Pt > NC	Middle Frontal Gyrus_R (Mask8)	0.044	Middle Frontal Gyrus_R (Mask8)	0.044
Pt > NC	Precentral Gyrus_L (Mask13)	0.044	Precentral Gyrus_R (Mask14)	0.035
Pt > NC	Precentral Gyrus_R (Mask14)	0.012	Postcentral Gyrus_L (Mask33)	0.035
Pt > NC	Postcentral Gyrus_L (Mask33)	0.027	Postcentral Gyrus_R (Mask34)	0.016
Pt > NC	Postcentral Gyrus_R (Mask34)	0.016	Superior Parietal Lobule_L (Mask35)	0.035
Pt > NC	Superior Parietal Lobule_L (Mask35)	0.012		
Pt < NC	Temporal Pole_R (Mask16)	0.044	Insular Cortex_R (Mask4)	0.016
Pt < NC	Planum Polare_L (Mask 87)	0.016	Temporal Pole_R (Mask16)	0.035
Pt < NC			Temporal Fusiform_L, anterior (Mask73)	0.035
Pt < NC			Planum Polare_L (Mask 87)	0.009

**Conclusions:** The fact that our preliminary results (e.g., abnormal regional glucose metabolism and prevalence of asymmetry) are consistent with the clinical data of epilepsy patients suggests that simultaneous PET/MR imaging provides a useful imaging tool to identify regional abnormality and assist in localizing the seizure focus.

### Reference

1) Di and Biswal, Brain Connectivity 2:275-283, 2012.

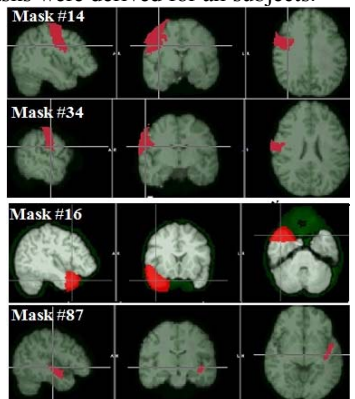


**Fig. 1.** Selected masks that showed group difference.

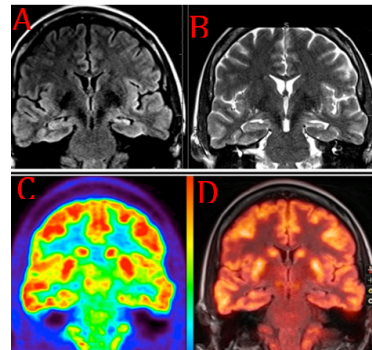


**Fig. 2. Top:** an epilepsy patient with left hippocampal sclerosis shown by coronal T2 FLAIR (A) and T2 (B). **Bottom:** (C) coronal FDG and (D) overlaid FDG with T2 FLAIR, showing good correlation of hypometabolism in the lesion area.

**Fig. 3.** Comparison of time-activity curves of this patient vs. a matched control in left hippocampus, consistent with patient's hypometabolism.

